

# Influence of autogeneous pressure under hydrothermal reaction on the structural and thermal stability of nanostructured titanates

Somjit Putdee<sup>a</sup>, Okorn Mekasuwandumrong<sup>b</sup>, Apinan Soottitantawat<sup>a</sup>, Joongjai Panpranot<sup>a,\*</sup>

<sup>a</sup>Center of Excellence on Catalysis and Catalytic Reaction Engineering, Department of Chemical Engineering, Faculty of Engineering, Chulalongkorn University, Bangkok 10330, Thailand

<sup>b</sup>Department of Chemical Engineering, Faculty of Engineering and Industrial Technology, Silpakorn University, Nakorn Pathom 73000, Thailand

Received 16 January 2013; received in revised form 1 August 2013; accepted 1 August 2013

Available online 29 August 2013

## Abstract

Synthesis of four different morphologies of nanostructured titanates (sphere (TNS), sponge (TNSp), tube (TNT) and wire (TNW)) by hydrothermal reaction was investigated under the presence/absence of autogeneous pressure. Starting from 5 m<sup>2</sup>/g anatase TiO<sub>2</sub> particles (com-TiO<sub>2</sub>), TNS and TNSp products with surface area > 200 m<sup>2</sup>/g were obtained under atmospheric pressure at 150 and 200 °C, respectively. On the other hand, TNT (192 m<sup>2</sup>/g) and TNW (23 m<sup>2</sup>/g) were synthesized at 150 and 200 °C under autogeneous pressure in a Teflon line autoclave reactor, respectively. After annealing at 600 °C, TNS, TNSp, and TNT transformed back into anatase TiO<sub>2</sub> but their surface areas were still much higher than the original one (60–70 m<sup>2</sup>/g). Annealing of the TNW resulted in metastable form TiO<sub>2</sub> under similar conditions with no significant change of the surface area.

© 2013 Published by Elsevier Ltd and Techna Group S.r.l.

**Keywords:** Hydrothermal; Titanate; Nanotube; Nanowire

## 1. Introduction

Owing to their enhanced specific surface area, mesopore volume, and cation-exchange capacity, nanostructured TiO<sub>2</sub> materials has been explored in several fields, such as catalysis, biochemistry, separation science, and sensors [1–7]. Since the innovative work of Kasuga et al. [8], who first synthesized uniform titanate nanotubes by hydrothermal reaction of crystalline TiO<sub>2</sub> in highly concentrated NaOH solution, many attempts have been made to elucidate the mechanism of this synthesis route and the factors determining the composition, crystal and textural structure of the resulting nanostructured materials [9,10]. Typically, four different morphologies of titanates were observed during alkaline hydrothermal treatment of TiO<sub>2</sub> including nanotubes (I), nanosheets (II), nanorods or nanowires (III), and nanofibers, nanoribbons, or nanobelts (IV). It has been suggested that under alkaline conditions, the observed intermediate single layer and multi-layered titanates nanosheets play a key role in the formation of tubular morphology [11,12]. These nanosheets can

scroll or fold into a nanotubular morphology. The driving force for curving these nanotubes has been considered by many groups. For examples, Zhang et al. [13] proposed a bending mechanism due to an asymmetrical chemical environment from the imbalance of H<sup>+</sup> or Na<sup>+</sup> ion concentration on two different sides of a nanosheet. Another reason for bending multilayered nanosheets is that mechanical tensions arise during the process of dissolution/crystallization in nanosheets [12].

Several parameters have been investigated, such as reaction time, reaction temperature, concentration of NaOH, average size of raw TiO<sub>2</sub> powder, post-synthesis heat-treatment temperature, and sonication pretreatment power [14–27], to find out their effects on morphology transformation, specific surface area, crystal structure, and so on. However, in those previous studies, the hydrothermal reaction occurred under autogeneous pressure. The morphology and structural properties of the nanostructured titanates formed in the absence of autogeneous pressure have seldom been reported.

In the present work, the synthesis of nanostructured titanates was carried out under the presence/absence of autogeneous pressure. Unlike the typical titanate nanotubes and nanowires, different titanate morphology such as nanosphere and sponge

\*Corresponding author. Tel.: +66 8303 65411; fax: +66 3421 9368.

E-mail address: [joongjai.p@chula.ac.th](mailto:joongjai.p@chula.ac.th) (O. Mekasuwandumrong).

can be obtained when  $\text{TiO}_2$  was treated in NaOH without autogeneous pressure. Physical properties and thermal stability of these nanostructure titanates were investigated using X-ray diffraction (XRD),  $\text{N}_2$  physisorption, scanning electron microscope (SEM), and transmission electron microscopy (TEM).

## 2. Experimental

### 2.1. Powder synthesis

Synthesis of nanostructured titanates was carried out by the hydrothermal method using anatase  $\text{TiO}_2$  (Com- $\text{TiO}_2$ , Sigma-Aldrich) as the starting material. First, 1.5 g of  $\text{TiO}_2$  powder was suspended in 40 ml of 10 M NaOH and then the mixture was sonicated for 10 min. Then, the mixture was transferred to a flask or Teflon-lined stainless steel autoclave, and heated at various reaction temperatures ranging from 150 to 200 °C for 24 h in an oven. After hydrothermal reaction, the autoclave was cooled to room temperature by natural cool down. The sample was washed with 0.1 M HCl for several times followed by deionized water until pH value approached that of the deionized water. Finally, the sample was dried at 110 °C for 24 h. The dried powder was annealed at 400, 500, and 600 °C for 1 h in air.

### 2.2. Powder characterization

XRD patterns were determined using a Siemens D5000 X-ray diffractometer using a Ni filtered  $\text{CuK}_\alpha$  radiation. The morphology and particle size were obtained using a Hitachi s-3400N scanning electron microscope and a JEOL-JEM 2010 transmission electron microscope. Specific surface area of the sample was measured by nitrogen gas adsorption at liquid nitrogen temperature (−196 °C) using a Micromeritics Chemi-Sorb 2750 system.

## 3. Results and discussion

The SEM micrographs of the as-synthesized powder are shown in Fig. 1. In the absence of autogeneous pressure, spherical shape particles (TNS) were formed after treatment at 150 °C. Further increasing hydrothermal temperature to 200 °C, sponge-like particles (TNSp) were obtained instead. On the other hand, hydrothermal treatment under autogeneous pressure, the as-synthesized sample showed fiber-like morphology. The length of the nanofibers formed at 150 °C was varied ranging from several 10  $\mu\text{m}$  to more than 100  $\mu\text{m}$ . Increasing hydrothermal temperature to 200 °C, the diameters of nanofibers were increased and the lengths became shorten. The TEM experiments were carried in order to investigate the true structure of these nanofibers (solid or hollow) and the results are shown in Fig. 2. The starting anatase  $\text{TiO}_2$  (Com- $\text{TiO}_2$ ) consisted of predominately spherical particles with average size around 100–200 nm. Moreover, the spherical TNS were in fact consisted of the agglomeration of nano-sized

particles. The as-synthesized nanofibers formed at 150 °C were hollow with the outer and inner diameter of the nanotubes (TNT) of approximately 10–12 nm and 4–6 nm, respectively. Increasing temperature to 200 °C led to the transformation of nanotubes to nanowire (TNW) with non-hollow morphology with a length of several micrometers and width varied between 60–100 nm. These results are in good agreement with the SEM images.

Fig. 3 shows the XRD patterns of the starting anatase  $\text{TiO}_2$  and the as-synthesized particles. The XRD patterns of all the hydrothermal-made products show the characteristic peaks of titanates with two main peaks at  $2\theta$  degrees 24.5° and 48.5° corresponding to the reflection (100) and (200) plane of H-titanate  $\text{H}_2\text{Ti}_x\text{O}_{2x+1}$ , probably trititanate ( $\text{H}_2\text{Ti}_3\text{O}_7$ ) [28]. No diffraction peaks of other impurities (such as starting anatase  $\text{TiO}_2$  and NaCl) were observed.

From the above results, the formation mechanism of nanostructure titante is different between the reaction systems with and without autogeneous pressure. Several researchers have studied the mechanism of the hydrothermal reaction between raw  $\text{TiO}_2$  and NaOH solution to form titanate nanostructure using both theoretical and experimental methods. There is a general agreement that the reaction proceeds through several stages [29–31], including the slow dissolution of raw  $\text{TiO}_2$  in NaOH solution accompanied by epitaxial growth of layered nanosheets of sodium titanates followed by the rolling up of exfoliated titanate sheets to form nanotube or nanorod samples. The driving force for the scrolling of the nanosheets into nanotubes has been proposed by Zhang et al. [4] including asymmetrical chemical environment on the two opposite sides of the nanosheet or the internal stress arising in the multilayered nanosheets from an imbalance in width, which occurred during the crystallization. Further increasing of reaction temperature resulted in the formation of nanorod structures due to the decreasing of nucleation and preferential crystal growth along the 010 direction of trititanate. However, this was probably not the case for the hydrothermal treatment without autogeneous pressure since there was a change in the nanostructure. It would start from the reaction between anatase  $\text{TiO}_2$  and NaOH solution where the small spherical particles of titanates were formed and aggregated to form larger particles with an equivalent size of the raw  $\text{TiO}_2$ . It seemed to be that the reaction took place on the surface of  $\text{TiO}_2$  to form small spherical particles and penetrate deep down inside the particles by diffusion. When the reaction temperature increased the sponge particles were formed. The reaction pathway to form nanostructure titanate under different conditions (with and without autogeneous pressure) is summarized in Scheme 1.

### 3.1. Thermal stability of nanostructure titanates

Another difficulty while utilizing nanostructure titanates is that the nanotubular structure of titanates is relatively unstable and can undergo further phase transformation upon heating, [27] acid treatment, [28] or other chemical treatments, during or after preparation of nanotubes. Thermal stability of the nanostructure titanate was investigated by calcining the as-synthesized product

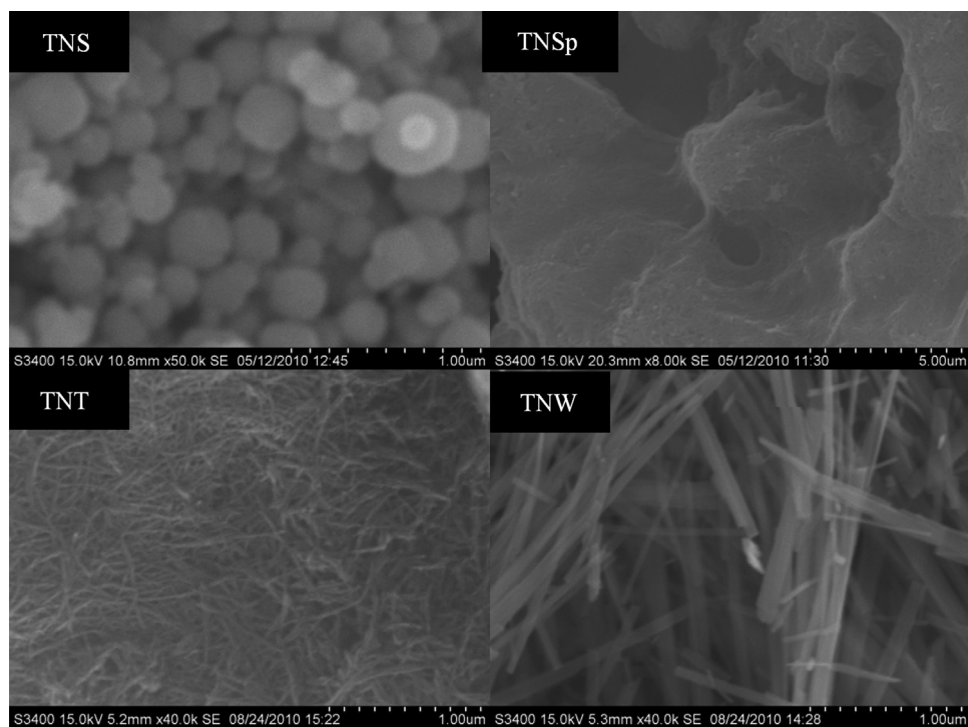


Fig. 1. SEM micrographs of the nanostructure titanate.

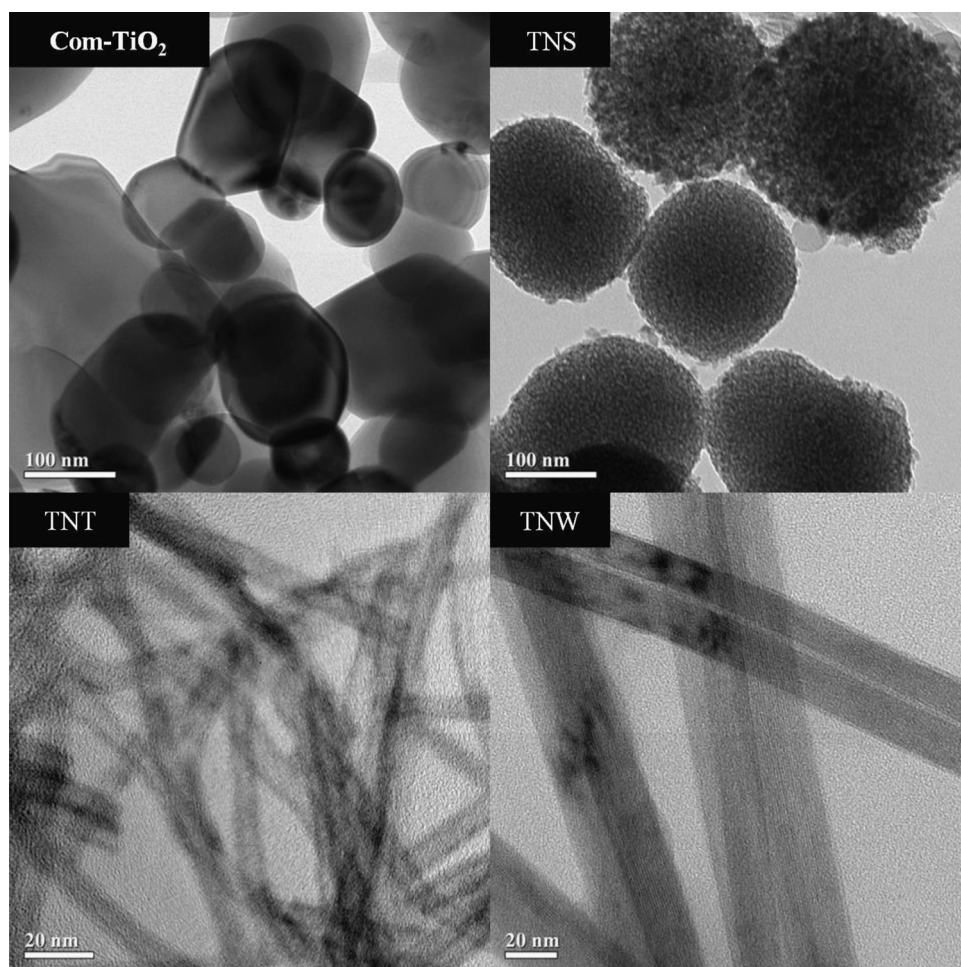


Fig. 2. TEM micrographs of the commercial TiO<sub>2</sub> and nanostructure titanate.



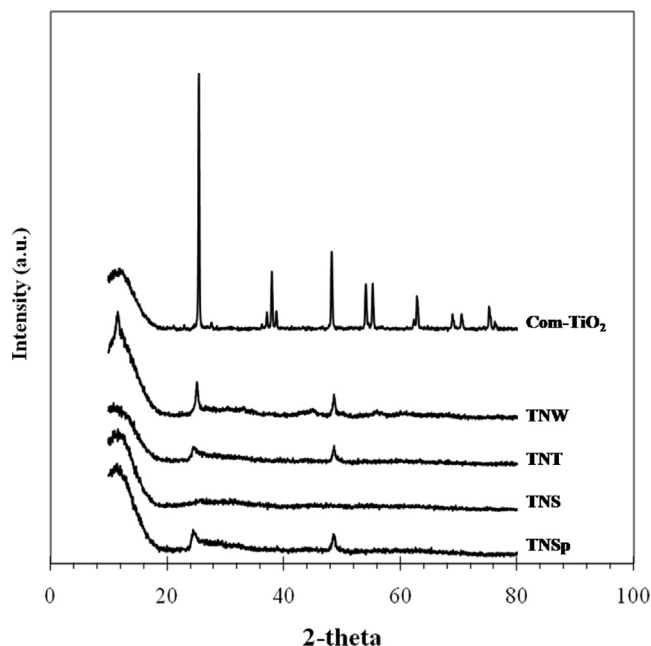
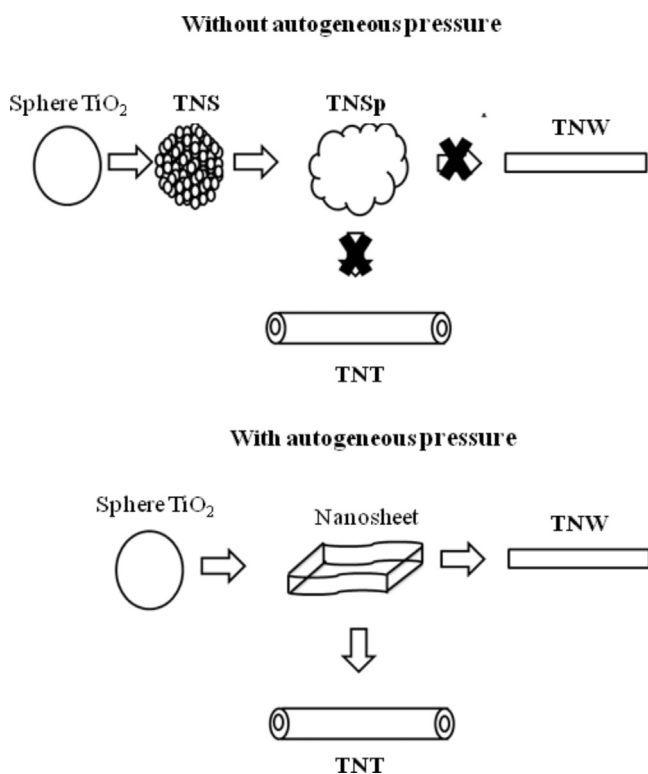


Fig. 3. XRD patterns of the commercial  $\text{TiO}_2$ .



Scheme 1. Titanate formation mechanism.

at various temperatures for 1 h. Fig. 4 shows the XRD patterns of the nanostructure titanates (sphere, sponge, tube, and rod) after annealing at 400–600 °C. The as-prepared powder exhibited poor crystalline quality. The crystalline structure of the sample was improved by thermal treatment. According to the XRD results, annealing spherical-shape, sponge-like, and

nanotube titanate at 400 °C resulted in the formation of anatase  $\text{TiO}_2$  phase. When the sample was annealed at 500 °C and 600 °C, the peak intensities corresponding to anatase  $\text{TiO}_2$  increased and the characteristic peaks of titanate disappeared. In other words, the titanate was completely transformed back to anatase  $\text{TiO}_2$ . For the titanate nanowires, after annealing at the temperature in the range of 400–600 °C, a metastable form of titanium dioxide was observed as shown in Fig. 4. It is suggested that the titanate nanowires were completely dehydrated and re-crystallized into metastable  $\text{TiO}_2$  ( $\text{TiO}_2\text{-B}$ ) [32]. Further increasing of the annealing temperature to 700 °C, the XRD pattern of anatase  $\text{TiO}_2$  was observed (the results not shown). This indicates that metastable  $\text{TiO}_2$  ( $\text{TiO}_2\text{-B}$ ) was transformed to anatase  $\text{TiO}_2$  at higher temperature.

The SEM images of the titanate nanostructure annealed at 600 °C are shown in Fig. 5. It can be seen that the morphologies of TNS and TNSp were not changed while TNT particles were shorter than the as-synthesized ones and some of them were converted to particles because the tubular structure was collapsed when annealed at relatively high temperature [31]. It should also be noted that the nanotube structure was not formed by annealing of the nanosheet or nanotube particles. This result suggests that the formation of the nanotube structure occurs under the reaction conditions with autogeneous pressure. TNW particles became larger due to the sintering process.

Fig. 6 illustrates the TEM images of annealed TNT and TNW. After thermal treatment at 600 °C, the nanotubes were partially broken and the hollow disappeared. The rod-like and some particles structure were observed. This is consistent to those previously reported regarding the conversion of the titanates into anatase  $\text{TiO}_2$  phase by thermal dehydration [33,34]. This is associated with the collapse of the interlayer spacing between the walls of the nanotubes, resulting in the anatase phase as confirmed by the XRD results. Therefore, it can be concluded that during annealing treatment at high temperature, the chemical bond such as  $\text{H}_2\text{O}$  and  $\text{-OH}$  were removed from the titanate nanotubes so that then it converted back to particles again. For TNW, the morphology was not significantly changed after thermal treatment at 600 °C.

Specific surface areas of the samples were determined from the  $\text{N}_2$  physisorption data using Brunauer–Emmett–Teller (BET) technique. Table 1 summarizes the BET surface area of all the titanates before and after calcination at 600 °C. The BET surface area of the Com- $\text{TiO}_2$  as the starting material was 5  $\text{m}^2/\text{g}$ . Hydrothermal treatment under atmospheric pressure at 150 °C resulted in a dramatically increased BET surface area to 211  $\text{m}^2/\text{g}$  whereas the samples treated under autogeneous pressure exhibited the BET surface area of 192  $\text{m}^2/\text{g}$ . Increasing of the BET surface areas was attributed to the morphology change to the nanostructure titanates that possessed higher surface area. The sample synthesized at 200 °C under autogeneous pressure had the lowest BET surface area (23.2  $\text{m}^2/\text{g}$ ) due to non-hollow structure of the TNW. After calcination at 600 °C, TNS, TNSp, and TNW transformed completely to anatase  $\text{TiO}_2$ , as a consequence the BET surface area decreased to 60–70  $\text{m}^2/\text{g}$ . It is interesting that even after phase

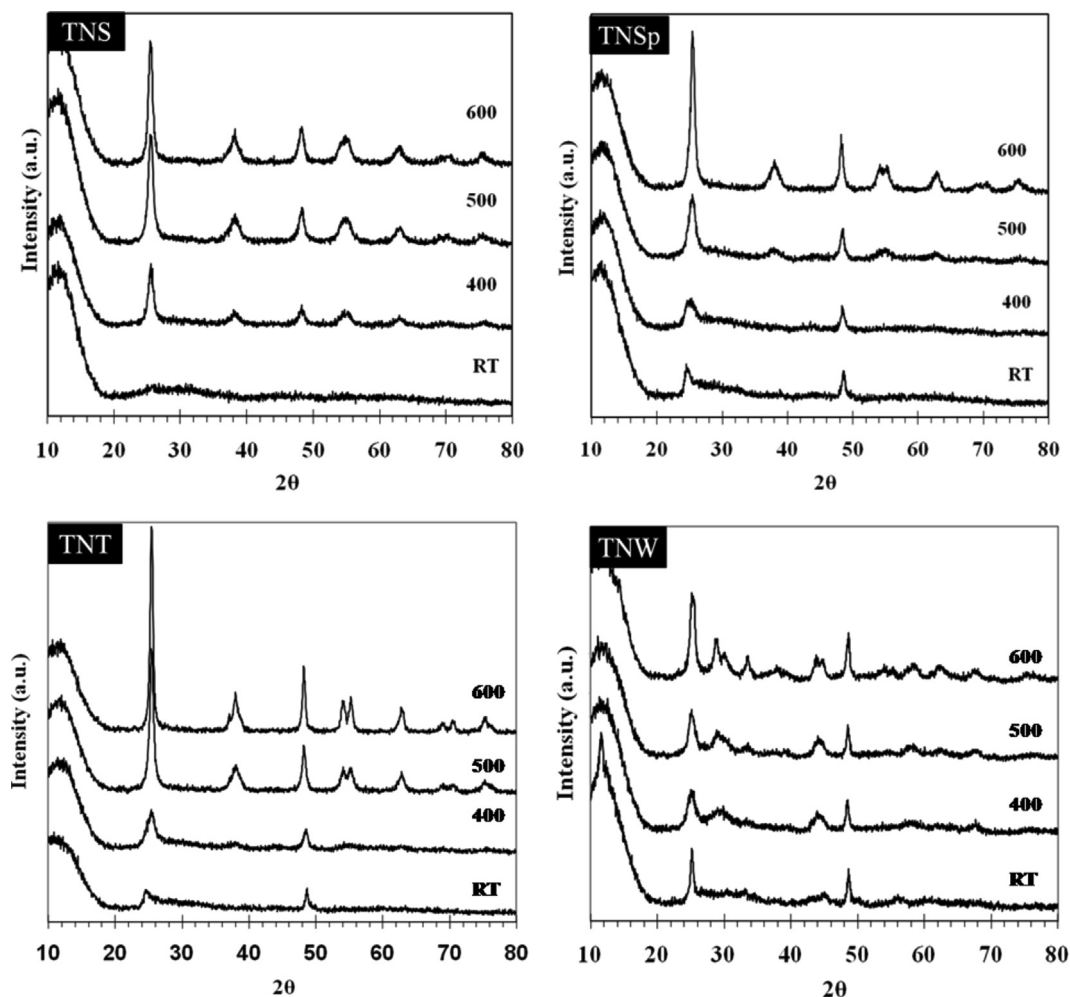


Fig. 4. XRD patterns of the nanostructure titanate after annealing at 400–600 °C.

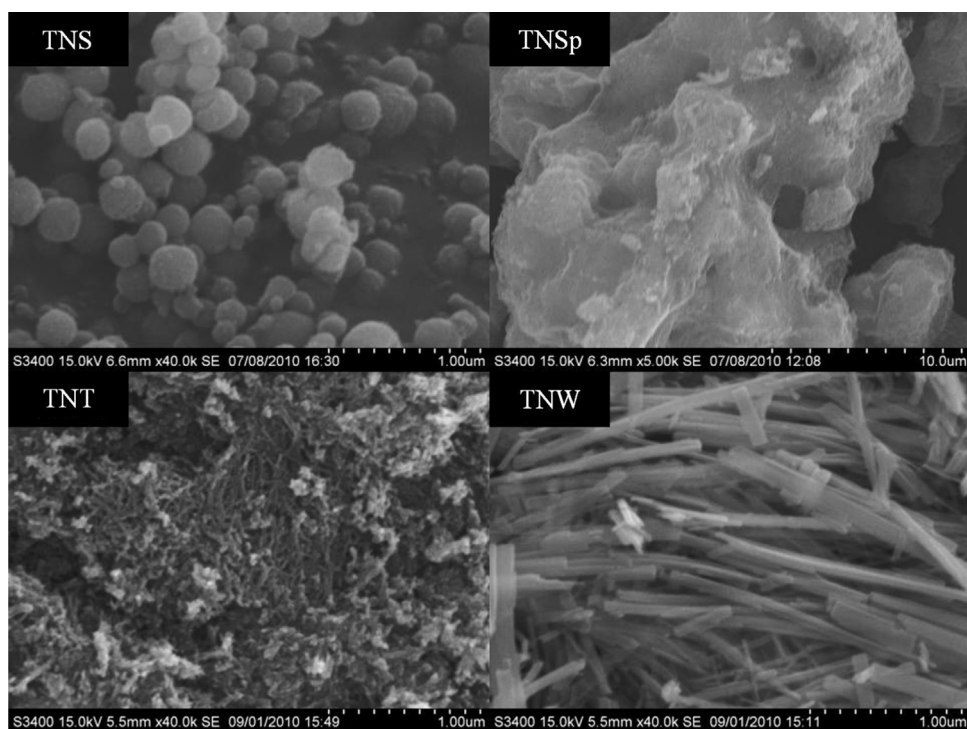


Fig. 5. SEM micrographs of the nanostructure titanate after annealing at 600 °C.

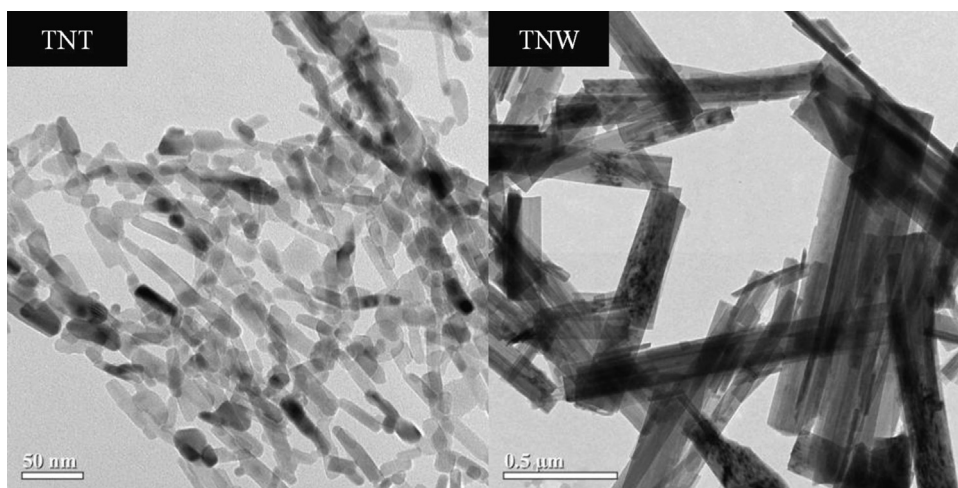


Fig. 6. TEM micrographs of the TNT and TNW after annealing at 600 °C.

Table 1  
BET surface area of nanostructure titanate before and after annealing at 600 °C.

Sample	BET surface area (m <sup>2</sup> /g)
TiO <sub>2</sub> commercial	4.8
<i>Teflon vessel</i>	
Spherical titanate (TNS)	211.1
TNS annealed 600 °C	71.7
Sponge titanate (TNSp)	211.9
TNSp annealed 600 °C	63.5
<i>Teflon-lined autoclave</i>	
Nanotube titanate (TNT)	192.0
TNT annealed 600 °C	63.0
Nanorod titanate (TNW)	23.2
TNW annealed 600 °C	19.4

transformation to anatase TiO<sub>2</sub>, the annealed samples still possessed very high BET surface area comparing to the starting Com–TiO<sub>2</sub>. However, phase transformation to anatase did not occur in the case of TNW and the BET surface area of annealed TNW sample was slightly changed.

#### 4. Conclusions

Four different morphologies of the nanostructure titanate (sphere (TNS), sponge (TNSp), tube (TNT) and wire (TNW)) were successfully synthesized by using hydrothermal reaction of a spherical shape anatase TiO<sub>2</sub>. The TNS and TNSp products with very high surface area (211 m<sup>2</sup>/g) were formed under atmospheric pressure at 150 and 200 °C, respectively. While the TNT and TNW products were synthesized at 150 and 200 °C under autogeneous pressure, respectively. The formation of TNT and TNW was started from the dissolution of raw TiO<sub>2</sub> in NaOH solution accompanied by epitaxial growth of layered nanosheets of sodium titanates followed by the rolling up of the exfoliated titanate sheets to form nanotube or nanorod samples. However, without autogeneous pressure, the mechanism was different. It would start from the reaction

between anatase TiO<sub>2</sub> and NaOH solution where small spherical particles of the titanates were formed and aggregated to form larger particles with an equivalent size of the raw TiO<sub>2</sub>. When the reaction temperature increased the sponge particles were formed instead. After annealing at 600 °C, TNS, TNSp and TNT transformed back into anatase TiO<sub>2</sub> whereas annealing of the titanate nanowires resulted in metastable form TiO<sub>2</sub> under similar conditions.

#### Acknowledgments

Financial supports from the Thailand Research Fund (TRF), the Office of Higher Education Commission, the National Council Research of Thailand (NRCT-JSPS Joint Research Program), and the NRU-CU (CU56-AM10) are gratefully acknowledged.

#### References

- [1] C.N.R. Rao, M. Nath, Inorganic nanotubes, *Dalton Transactions* 1 (2003) 1–24.
- [2] O.K. Varghese, D. Gong, M. Paulose, K.G. Ong, C.A. Grimes, Hydrogen sensing using titania nanotubes, *Sensors and Actuators B* 93 (2003) 338–344.
- [3] M. Huang, S. Mao, H. Feick, H. Yan, Y. Wu, H. Kind, E. Weber, R. Russo, P. Yang, Room-temperature ultraviolet nanowire nanolasers, *Science* 292 (2001) 1897–1899.
- [4] B. Zhang, F. Chen, W.W. Qu, J.L. Zhang, The evolution of pits and dislocations on TiO<sub>2</sub>-B nanowires via oriented attachment growth, *Journal of Solid State Chemistry* 182 (2009) 2225–2230.
- [5] H.Y. Zhu, Y. Lan, X.P. Gao, S.P. Ringer, Z.F. Zheng, D.Y. Song, J.C. Zhao, Phase transition between nanostructures of titanate and titanium dioxides via simple wet-chemical reactions, *Journal of the American Chemical Society* 127 (2005) 6730–6736.
- [6] D.J. Yang, Z.F. Zheng, H.Y. Zhu, H.W. Liu, X.P. Gao, Titanate nanofibers as intelligent absorbents for the removal of radioactive ions from water, *Advanced Materials* 20 (2008) 2777–2781.
- [7] J.Q. Huang, Z. Huang, W. Guo, M.L. Wang, Y.G. Cao, M.C. Hong, Facile synthesis of titanate nanoflowers by a hydrothermal route, *Crystal Growth and Design* 8 (2008) 2444–2446.
- [8] T. Kasuga, M. Hiramatsu, A. Hoson, T. Sekino, K. Niihara, Formation of titanium oxide nanotube, *Langmuir* 14 (1998) 3160–3163.

- [9] C.H. Han, D.W. Hong, I.J. Kim, J. Gwak, S.D. Han, K.C. Singh, Synthesis of Pd or Pt/titanate nanotube and its application to catalytic type hydrogen gas sensor, *Sensors and Actuators B* 128 (2007) 320–325.
- [10] N. Viriya-empikul, T. Charinpanitkul, N. Sano, A. Soottitawat, T. Kikuchi, K. Faungnawakij, W. Tanthapanichakoon, Effect of preparation variables on morphology and anatase–brookite phase transition in sonication assisted hydrothermal reaction for synthesis of titanate nanostructures, *Materials Chemistry and Physics* 118 (2009) 254–258.
- [11] R. Ma, Y. Bando, T. Sasaki, Directly rolling nanosheets into nanotubes, *Journal of Physical Chemistry B* 108 (2004) 2115–2119.
- [12] D.V. Bavykin, V.N. Parmon, A.A. Lapkin, F.C. Walsh, The effect of hydrothermal conditions on the mesoporous structure of  $\text{TiO}_2$  nanotubes, *Journal of Materials Chemistry* 14 (2004) 3370–3377.
- [13] S. Zhang, L.-M. Peng, Q. Chen, G.H. Du, G. Dawson, W.Z. Zhou, Formation mechanism of  $\text{H}_2\text{Ti}_3\text{O}_7$  nanotubes, *Physical Review Letters* 91 (2003) 256103.
- [14] T. Kasuga, M. Hiramatsu, A. Hoson, T. Sekino, K. Niihara, Titania nanotubes prepared by chemical processing, *Advanced Materials* 11 (1999) 1307–1311.
- [15] D.S. Seo, J.K. Lee, H. Kim, Preparation of nanotube-shaped  $\text{TiO}_2$  powder, *Journal of Crystal Growth* 229 (2001) 428–432.
- [16] Z.Y. Yuan, B.L. Su, Physicochemical and engineering aspects, *Colloid Surface A* 241 (2004) 173–183.
- [17] B. Poudel, W.Z. Wang, C. Dames, J.Y. Huang, S. Kunwar, D.Z. Wang, D. Banerjee, G. Chen, Z.F. Ren, Formation of crystallized titania nanotubes and their transformation into nanowires, *Nanotechnology* 16 (2005) 1935–1940.
- [18] R. Yoshida, Y. Suzuki, S. Yoshikawa, Syntheses of  $\text{TiO}_2(\text{B})$  nanowires and  $\text{TiO}_2$  anatase nanowires by hydrothermal and post-heat treatments, *Journal of Solid State Chemistry* 178 (2005) 2179–2185.
- [19] S. Pavasupree, S. Ngamsinlapasathian, Y. Suzuki, S. Yoshikawa, Preparation and characterization of high surface area nanosheet titania with mesoporous structure, *Materials Letters* 61 (2007) 2973–2977.
- [20] L.Q. Weng, S.H. Song, S. Hodgson, A. Baker, J. Yu, Synthesis and characterization of nanotubular titanates and titania, *Journal of the European Ceramic Society* 26 (2006) 1405–1409.
- [21] R. Ma, K. Fukuda, T. Sasaki, M. Osada, Y. Bando, Structural features of titanate nanotubes/nanobelts revealed by raman X-ray absorption fine structure and electron diffraction characterizations, *Journal of Physical Chemistry B* 109 (2005) 6210–6214.
- [22] Y. Ma, Y. Lin, X. Xiao, X. Zhou, X. Li, Sonication–hydrothermal combination technique for the synthesis of titanate nanotubes from commercially available precursors, *Materials Research Bulletin* 41 (2006) 237–243.
- [23] N. Viriya-empikul, N. Sano, T. Charinpanitkul, T. Kikuchi, W. Tanthapanichakoon, A step towards length control of titanate nanotubes using hydrothermal reaction with sonication pretreatment, *Nanotechnology* 19 (2008) 035601.
- [24] J. Yang, Z. Jin, X. Wang, W. Li, J. Zhang, S. Zhang, X. Guo, Z. Zhang, Study on composition, structure and formation process of nanotube  $\text{Na}_2\text{Ti}_2\text{O}_4(\text{OH})_2$ , *Dalton Transactions* 20 (2003) 3898–3901.
- [25] W. Chen, X. Guo, S. Zhang, Z. Jin, TEM study on the formation mechanism of sodium titanate nanotubes, *Journal of Nanoparticle Research* 9 (2007) 1173–1180.
- [26] Y.H. Zhu, Y. Lan, P.X. Gao, P.S. Ringer, F.Z. Zheng, Y.D. Song, J.C. Zhao, Phase transition between nanostructures of titanate and titanium dioxides via simple wet-chemical reactions, *Journal of the American Chemical Society* 127 (2005) 6730–6736.
- [27] J. Yu, H. Yu, Facile synthesis and characterization of novel nanocomposites of titanate nanotubes and rutile nanocrystals, *Materials Chemistry and Physics* 100 (2006) 507–512.
- [28] Y. Suzuki, S. Pavasupree, S. Yoshikawa, R. Kawahata, Natural rutile-derived titanate nanofibers prepared by direct hydrothermal processing, *Journal of Materials Research* 20 (2005) 1063–1070.
- [29] L. Torrente-Murciano, A.A. Lapkin, D.V. Bavykin, F.C. Walsh, K. Wilson, Highly selective Pd/titanate nanotube catalysts for the double-bond migration reaction, *Journal of Catalysis* 245 (2007) 272–278.
- [30] H.-K. Seo, G.-S. Kim, S.G. Ansari, Y.-S. Kim, H.-S. Shin, K.-H. Shim, E.K. Suh, Study on the structure/phase transformation of titanate nanotubes synthesized at various hydrothermal temperatures, *Solar Energy Materials and Solar Cell* 92 (2008) 1533–1539.
- [31] Y. Hou, H. Zheng, Z. Ding, L. Wu, Effects of sintering temperature on physicochemical properties and photocatalytic activity of titanate nanotubes modified with sulfuric acid, *Powder Technology* 214 (2011) 451–457.
- [32] S. Pavasupree, Y. Suzuki, S. Yoshikawa, R. Kawahata, Synthesis of titanate,  $\text{TiO}_2(\text{B})$ , and anatase  $\text{TiO}_2$  nanofibers from natural rutile sand, *Journal of Solid State Chemistry* 178 (2005) 3110–3116.
- [33] Z.Y. Yuan, B.L. Su, Titanium oxide nanotubes, nanofibers and nanowires, *Physicochemical and Engineering Aspects* 241 (2004) 173–183.
- [34] C.K. Lee, C.C. Wang, M.D. Lyu, L.C. Juang, S.S. Liu, S.H. Hung, Effects of sodium content and calcination temperature on the morphology, structure and photocatalytic activity of nanotubular titanates, *Journal of Colloid and Interface Science* 316 (2007) 562–569.